

## **P12A.2**

# **Aerosol and Thermodynamic Controls on Tropical Cloud Systems During TWPICE and ACTIVE**

Peter May

Bureau of Meteorology Research Centre,  
GPO Box 1289, Melbourne, 3001, Victoria, AUSTRALIA

Geraint Vaughan, Grant Allen, Tom Choularton and Paul Connolly  
University of Manchester

### **Introduction and background**

There has been considerable debate in the community concerning the impacts of aerosols on convective clouds. This has come about from a number of modelling and observational studies.

The Darwin area is an excellent location to test some of these ideas. In the build and breaks in the monsoon there is strongly locally forced thunderstorms. In particular, the “Hector” storms over the Tiwi Islands form on most days unless there is extensive cloud cover from overnight storms. The forcings for these storms, being the sea breeze and the relatively weak low level mean flow is reasonably constant. However, these storms form in a wide variety of thermodynamic and aerosol environments. The thermodynamics can be estimated/parameterised using the soundings from Darwin airport (ARCS site).

There is a strong seasonal dependence of aerosol characteristics. Early in the build up the atmosphere is very smoky with wide spread biomass burning. As the build up continues these fires decrease, but the low level continental flow ensures that aerosol concentrations remain reasonably high. The build up is followed by active monsoon periods. However, the aerosol loading during breaks in the monsoon, when thermodynamic and convective characteristics return to build up types, are very low.

The boundary layer aerosol has been quantified by the UK ACTIVE consortium, both during the build up from mid November to mid December 2005 and the core TWPICE period (Jan 20-Feb 14, 2006) using the UK Dornier aircraft. The aerosol instrument payload is discussed in detail in Appendix 1. The last week of TWPICE experienced break conditions. These data can be used to characterise three aerosol regimes:

Polluted: November 10-30 with significant black carbon and organics.

Moderate: December 1-26 with aerosol being mainly organics

Clean: February 6-26 where aerosol composition measurements on the Dornier aircraft were lower

than instrument sensitivity and an order of magnitude lower in concentrations.

This leads naturally to the question is it possible to detect significant variations in storm characteristics in different “aerosol regimes”?

### **Data and Methodology**

Four sources of data are used here. One is the aircraft measurements already discussed, the Darwin radiosonde soundings, MT-Sat1R brightness temperatures and the gridded radar reflectivity and microphysical classification data set generated from C-Pol data that is supplied to ARM.

The sounding data is analysed by the forecasters and an estimate of the Convective Available Potential Energy (CAPE) is produced from these samples every morning for both inland and coastal locations. This estimate is made using a “modified sounding” where the forecasters adjust the parcel characteristics. This has to be done because the radiosonde is launched at 9 am LT and allowance needs to be made for heating and moistening from surface fluxes and the consequent growth and mixing of the BL and entrainment processes. This procedure is widely employed around the world. We have used the operational estimate of “coastal CAPE” for the analysis so far as this is likely to be most appropriate for the Tiwi Islands.

The “C-Pol” radar is a 5.5 cm wavelength scanning polarimetric weather radar system presently located at Gunn Point (12.25°S, 131.04°E) near Darwin approximately 25 km to the north east of the Darwin ARCS site. As such it provides ARM both unique data for providing context for the column data collected at the ARCS site. A polarimetric radar has at least two significant capabilities compared with conventional radar. Firstly it is possible to measure rainfall much more accurately. This is because you can use rainfall estimators optimised for different rainfall rates including using information of the underlying drops size distributions and correct for the effects of radar attenuation. The second major capability is the determination of hydrometeor species. Different hydrometeors occupy different parts of the [ $Z_H$ ,  $Z_{DR}$ ,  $K_{DP}$ ,  $\rho_{HV}(0)$ , temperature]

phase space so the combination of parameters can be used with good success (e.g. May and Keenan, 2005).

An approach is to obtain height resolved statistics from the gridded data is to calculate the fraction of a domain that is covered by radar echoes greater than a range of reflectivity values as well as the fractional coverage of rain, snow etc and the height profile of the maximum reflectivity within the domain. It should be remembered that the C-Pol volume coverage is approximately a current GCM grid box size so that statistics gathered on this scale have direct relevance to modelling. However, two factors suggest augmenting this “whole domain” statistic. One is the size of GCM boxes is expected to approach 50 km over the next decade and second is the spatial in-homogeneity of the Darwin site that has already been alluded to in Fig 1. Thus we have been collecting these statistics for the whole domain and a number of sub-domains.

## Results

In order to look at this question of aerosol impacts from a purely observational point of view we have taken MT-Sat IR data and C-Pol data for a rectangular box that encloses the Tiwi Islands.

Time series of the area covered by cold cloud (i.e TB < -70, -50 and -30° C), as well as the area covered by rain, the 40dBZ area (the convective area), 10 dBZ (radar detectable anvil area) and other parameters such as hail area, the maximum height of the 20, 30 and 40 dBZ echoes and the maximum value of reflectivity anywhere for several Hector days. Days when there was no clear Hector or where the situation was complicated by squall lines etc were excluded. Time windows of 2-12 UTC for the satellite data and 0-12 UTC for the radar data are used, but the peaks are never before 2 UTC.

The value and time of the maximum area for each of these cloud/precipitation parameters are then calculated for the three regimes. There are 44 Hector cases in the sample and the data are stratified according to date (as per the introduction) as a proxy for aerosol loading, and with respect to the operational estimate for the Darwin CAPE to give some independent thermodynamic information. There are approximately equal numbers of cases in each period (9-14). Inevitably some parameters are more useful than others. For example the maximum reflectivity was always approximately 63 dBZ and there were always some 20 dBZ echoes overshooting the tropopause.

Fig 2. shows the mean and standard deviation of the maximum values discussed above as well as the timing. The timing of these maxima is fairly uniform for each of the variables being considered (not shown). It is remarkable that there is very little difference in the means of the 40 dBZ areas, the anvil areas (10 dBZ) and several other parameters not shown such as or the maximum reflectivities and hail area across the three aerosol regimes. There were two parameters that do show significant differences.

The height of the 40 dBZ echoes is on average lower in the clean regime. This is a proxy for updraft strength. The other significant difference was in the greater maximum rain area in the clean environment. The rain max occurs a bit later in the clean cases and after the convective max, but before the anvil max. The similarity of the 40 dBZ area and the lag implies that the enhanced rain area is associated with stratiform rain. An obvious question is if these signatures related to aerosols? It seems that the rain area is an unlikely candidate as the anvil areas were similar. One mechanism for a larger stratiform rain area compared with anvil area is if the mid-levels were significantly moister reducing evaporation of the settling ice particles. Analysis of the soundings does indeed show that on average the mid-level moisture is higher during the break than in the build up periods, although still much less than during the monsoon. This may also affect the dynamics. Drier mid-levels may enhance downdraft strength which in turn provide stronger forcing for new updrafts, so the picture is somewhat complicated. However, the aerosol may also affect the cloud particle nucleation which in turn may affect the updraft strength through changes in the balance between warm rain and ice dominated processes. It is interesting to note that another proxy for updraft strength, particularly near the freezing level is the hail area and this was uniform. Thus if the 40 dBZ is a proxy for updraft strength, it seems to be illustrating effects above the freezing level.

In terms of IR cloud cover the clean cases all sit between the early, high aerosol and the moderate post mini-monsoon periods. Times are almost identical, but this is hourly data. A question is are the smaller cloud areas early on associated with aerosol or upper level moisture given the radar statistics for the anvil look similar. The satellite data is sensitive to smaller particles so these may vary according to aerosol or may be affected by upper level moisture.

The lack of clear aerosol signatures begs the question if thermodynamic controls can be identified. If we examine a histogram of the CAPE data for the Hector days, we see a clear bi-modal distribution. This we can examine high and low CAPE storms separately. For CAPE we have stratified the data as > or < 2500 J/kg. It is worth noting that the above results are not substantially affected if only high CAPE cases are included in the aerosol regime analysis.

If we stratify by CAPE, bearing in mind the vagaries and sensitivities of CAPE given its sensitivity to the characteristics of the low level parcel (e.g. Weckwerth, 2000) and keeping in mind these are CAPE estimates for a forecast parcel as well as the small number of low CAPE cases we do see some distinct signal in the distributions. There is clearly a distinct stratification of the statistics in the radar summaries. There is substantial spread, but the area covered by rain, convection and anvil and height of the 40 dBZ echoes are all greater for the higher CAPE values and the maxima all occur earlier in the day than for the low CAPE cases. Despite this, the satellite data distributions look essentially identical.

## Discussion

This analysis has examined the statistics of thunderstorms that occurred over the Tiwi Islands during the build up and break phases of the 2005/6 wet season. There was a clear progression of aerosol loadings during this period, but several of the average storm characteristics were hardly affected. The exceptions to this were the 40 dBZ height and rain area. The rain area was most likely associated with systematic variations in mid-level moisture, but the storm intensity is more complex with both aerosol and thermodynamic effects possibly implicated. There needs to be detailed modelling performed to resolve this issue. The satellite statistics did show a mean coverage that was greater in the latter part of the build up with moderate aerosol. This may be consistent with some CRM results that there is an optimal level of aerosol for convective development. However, the distributions are strongly overlapping and similar signatures were not seen in the radar data. There was a significant signature if the data was stratified into low and high CAPE cases. Additional parameters that are being examined are the rain amounts and convective fraction of the rain.

Appendix 1. Aerosol Observations from the NERC Dornier (after Allen et al, JGR, Submitted manuscript)

### 2.1. Aerosol Instrumentation

Number and size: Aerosol particle number size distributions from 55 nm to 20  $\mu\text{m}$  diameter were measured using a range of optical probes (see Table 1). Herein, the terms fine mode and coarse mode aerosol refer to the sub-micron and super-micron aerosol population fraction. Optical scattering instruments included:

(i) a Droplet Measurement Technologies (DMT, Boulder, CO, UK) ultra high sensitivity aerosol spectrometer (UHSAS) measuring dry fine mode aerosol size spectra at 1 Hz (averaged to 1/6 Hz) with a fine size resolution (7.5 nm bins) in the range 55 nm to 800 nm.

(ii) A prototype DMT aerosol spectrometer probe (ASP) measuring dry size ranges with a resolution between 0.1 and 0.2  $\mu\text{m}$  in the range 0.3 to 25  $\mu\text{m}$ ;

(iii) A Grimm Aerosol Technik (GmbH) 1.108 optical particle counter (Ainring, Germany) measuring dry size ranges with a resolution between 0.03 and 0.5  $\mu\text{m}$  in the range 0.21 to 4.5  $\mu\text{m}$ .

(iv) For the coarse aerosol component, a wing-mounted forward scattering spectrometer probe (FSSP-100), described further by Baumgardner et al., (1985), measuring ambient particle number size distributions with resolution 0.8  $\mu\text{m}$  from 0.5 to 32  $\mu\text{m}$ .

In addition, a TSI-3010D (TSI Inc., Shoreview, MN, USA) condensation particle counter (CPC) measured the total particle number concentration greater than  $\sim 10$  nm. However, absolute number concentrations for sizes greater than 2  $\mu\text{m}$  measured by the ASP and Grimm instruments are not considered here due to

inlet transmission limitations (50% transmission at 2  $\mu\text{m}$ )

Black carbon: A Radiance Research Inc particle soot absorption photometer (PSAP) measured black carbon content. For this study, the soot absorption cross-section ( $\sigma_{ae} = 8.2 \text{ m}^2\text{g}^{-1}$ ) used by Ben Liley et al., (2003), for the geographically similar BIBLE campaign is assumed. To account for high measurement noise, 0.2 Hz PSAP data were smoothed over a five-minute period. In stable operating conditions the PSAP sensitivity to changes in filter absorption gives a precision of  $10^{-6} \text{ m}^{-1}$ , or roughly  $0.02 \mu\text{g m}^{-3}$  of soot for five-minute integration.

Composition: A Quadrupole Aerodyne Aerosol Mass Spectrometer (Q-AMS) system (Jayne et al., 2000), which sampled air through the main manifold, was used to determine the mass loading of the non-refractory, non sea-salt chemical component of sub-micron aerosol with a high time resolution (30 seconds). This instrument employs thermal desorption, 70 eV electron ionisation, and a quadrupole mass spectrometer. Data were processed and quality assured using the procedures described by Jimenez et al., (2003) and Allan et al., (2003; 2004) and employed in conjunction with the pressure-dependent calibrations and corrections described by Crosier et al., (2006) needed for aircraft operation. Mass concentrations are reported from the Q-AMS (see Section 5) for the total nitrate, organic, sulphate and ammonium component masses in the aerosol. Component mass size distributions could not be derived here with sufficient confidence (reasonable signal to noise) due to the relatively clean environment sampled throughout the majority of ACTIVE flights.

## References

Allan, J. D., Jimenez, J. L., Williams, P. I., Alfarra, M. E., Bower, K. N., Jayne, J. T., Coe, H., and Worsnop, D. R., 2003: Quantitative sampling using an Aerodyne Mass Spectrometer 1, Techniques of data interpretation and error analysis, *J. Geophys. Res.-Atmos.*, 108, 4090-4099.

Allan, J. D., Coe H., Bower, K. MN., Alfarra, M. R., Delia, A. E., Jimenez, J. L., Middlebrook, A. M., Drewnick, F., Onasch, T. B., Canagaratna, M. R., Jayne, J. T., and Worsnop, D. R., 2004: A generalised method for the extraction of chemically resolved mass spectra from Aerodyne aerosol mass spectrometer data, *J. Aerosol. Sci.*, 35, 909-922.

Ben Liley, J., Baumgardner, D., Kondo, Y., Kita, K., Blake, D. R., Koike, M., Machida, T., Takegawa, N., Kawakami, S., Shirai T. and Ogawa, T., 2003: Black carbon in aerosol during BIBLE B, *J. Geophys. Res.*, 108, 8399

Jimenez, J. L., Jayne, J. T., Shi Q., et al., 2003: Ambient aerosol sampling using the Aerodyne Mass Spectrometer, *J. Geophys. Res.*, 108, 8425-8437.

May, P.T. and T.D. Keenan, 2005: Evaluation of microphysical retrievals from polarimetric radar with wind profiler data, J. Appl. Meteor. 44, 827–838.

Weckwerth, T.M., 2000: The effect of small-scale moisture variability on thunderstorm initiation. Mon. Wea. Rev., 128, 4017–4030

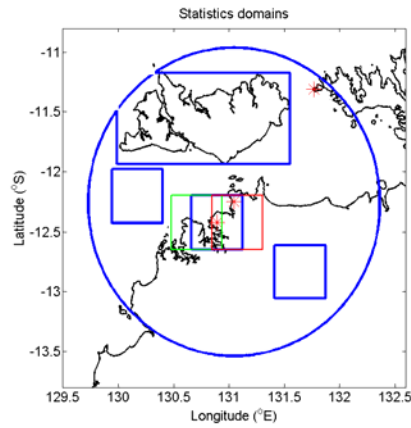


Fig 1. Domains for the collection of level 3 product statistics. These are the fractional of the domain covered by reflectivity greater than [0, 10, 20, 30, 40, 50] dBZ, covered by rain, snow, graupel, and hail as well as the maximum reflectivity in the domain as a function of height and time. This manuscript focussed on the northern box over the Tiwi islands.

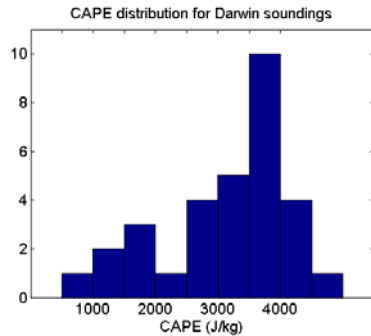


Figure 2. Distribution of CAPE estimated from operational Darwin soundings for the Hector days.

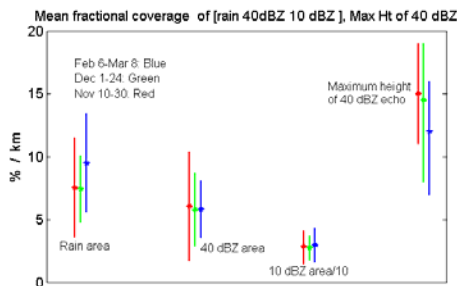


Fig 3. Mean and standard deviation of the maximum area covered by rain, the time of that maximum, maximum area covered by 40 dBZ, the maximum area covered by 10 dBZ divided by 10, and the maximum height of the 40 dBZ echo for a given day. The three values for each are for high, moderate and low aerosols as sorted by date.

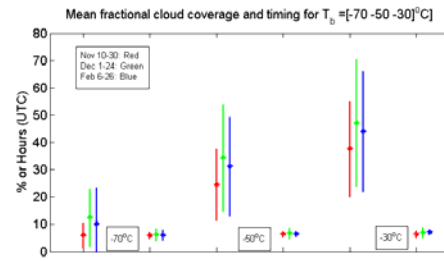


Fig 4. Mean and standard deviation of the maximum fractional coverage and time of that maximum for  $T_b$  of -70, -50 and -30 °C.

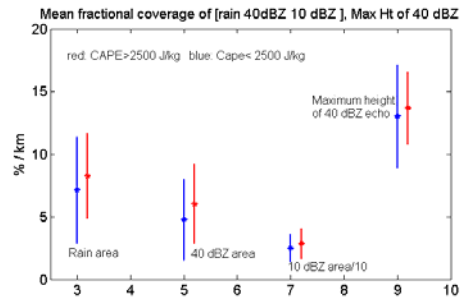


Figure 5 As Fig. 3 except stratified by the operational estimate of CAPE from Darwin soundings.

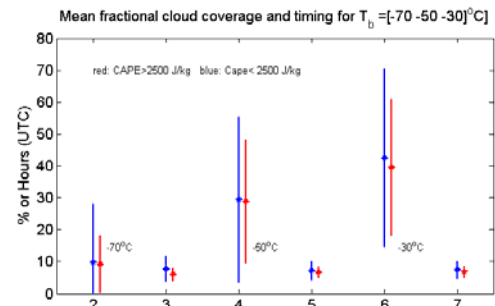


Figure 6 As for Fig 4, but for data stratified by CAPE.